Research Article

Propagation of Shear Horizontal Wave at Magneto-Electro-Elastic Structure Subjected to Mechanically Imperfect Interface

Anandakrishnan Akshaya, Santosh Kumar *, Kulandhaivel Hemalatha

Department of Mathematics, College of Engineering and Technology, SRM Institute of Science and Technology, Kattankulathur-603203, INDIA

ARTICLE INFO

ABSTRACT

This study delves into the investigation of shear horizontal transverse waves within a structure composed of a layer and a semi-infinite medium. The layer considered in this work is made of functionally graded magneto-electro-elastic material, and the semi-infinite medium is comprised of functionally graded piezoelectric material with a linear gradedness parameter. Additionally, the layer and semi-infinite medium has a mechanical imperfect interface. Furthermore, the solutions for the layer and semi-infinite medium are derived utilizing the WKB approximation technique. This involves initially transforming the partial differential equation into an ordinary differential equation through basic variable separation and the ordinary differential equation is solved by WKB approximation technique. The obtained results lead to dispersion relations presented in determinant form for two cases: electrically open and short. To explore the influences of various parameters on shear horizontal transverse waves, a specific model is considered. This model is composed of a layer made of magneto-electro-elastic material ($BaTiO_3$-$CoFe_2O_4$) and a semi-infinite medium consisting of piezoelectric material ($BaTiO_3$). Also, the graphs are plotted to visualize the variation in shear horizontal transverse waves in relation to both phase velocity and wave number.

1. Introduction

The investigation into the propagation of shear horizontal transverse waves within a structure, comprising magneto-electro-elastic layers and piezoelectric material, constitutes an intriguing research area with diverse real-world applications such as surface acoustic wave devices [1], ultrasound imaging [2], and so on. Shear horizontal transverse waves arise from disturbances within a medium capable of storing and transmitting energy. The origin of these disturbances can be attributed to various mechanisms contingent upon the characteristics of the medium. The analyzed layer, comprising magneto-electro-elastic materials, serves as a smart composite with the ability to convert mechanical energy to electric or magnetic energy, and vice versa. The electromagnetic coupling effect occurs in magneto-electro elastic materials, involving the interaction between electric and magnetic fields within the material, which gives rise to their piezoelectric and piezomagnetic properties. The piezomagnetic substance undergoes a change in its magnetic properties

* Corresponding author.
  E-mail address: santosh453@gmail.com

when subjected to external mechanical stress. It is possible to convert energy between electric and magnetic fields with the use of composite materials that include both piezo-magnetic and piezo-electric. This study focuses specifically on piezoelectric materials [3], recognized for their widespread use in everyday items such as touch-sensitive lighters, as well as in applications like microphones, sensors, motors, and various other technological devices.

One may produce a spontaneous magnetic moment in a piezomagnetic material by subjecting it to mechanical stress, and one can induce a physical deformation by subjecting it to a magnetic field. Li and Wei [4] studied the impact of short and open circuits as well as piezoelectric and piezomagnetic effects, on the speed of surface waves in a half-infinite magneto-electro-elastic material. Harmonic wave propagation on magneto-electro-elastic multilayered plates was the subject of an analytical analysis published by Chen et al. [5], who also expanded on their previous work on multilayered plates with nonlocal effects [6]. Akshaya et al. [7] analyzed the transference of SH-wave in two different functionally graded half-spaces bonded imperfectly. Liu et al. [8] investigated the Love wave propagation across layered structures, looking at the situation in which a piezomagnetic (PM) layer lies above a piezoelectric half-space. Akshaya et al. [9] investigated the behavior of transverse waves at an imperfectly corrugated interface within a functionally graded structure. Yang et al. [10] studied the phenomenon of SH waves being scattered by splits in infinite magneto-electro-elastic materials. Li et al. [11] studied the SH wave at the stress-free surface of a functionally graded magneto-electro-elastic material subjected to initial stress. Hemalatha et al. [12] explored SH waves in a pre-stressed anisotropic magnetoelastic layer interacting with heterogeneous half-spaces.

The functional gradient material is a new kind of material whose characteristics vary with the variation in space. The designed piezoelectric material is crafted to exhibit specific features for a particular application, regularly modified in an appropriate direction with respect to both the structure and the material's properties. Several new studies [13-16] have been carried out on how Love waves move through a layered composite FGPM system. There have also been efforts to draw attention to the effect that material gradients have on the frequency curves of the examined surface waves. The behavior of Love waves as they travel through a semi-infinite, quadratically changing, functionally graded piezoelectric material is discussed by Eskandari and Shodja [17]. Akshaya et al. investigated the reflection and transmission coefficients of SH

waves in a functionally graded piezoelectric structure. The behavior of Love waves during propagation in a three-layered composite structure subjected to initial stress was analyzed by Saroj et al. [19]. In Singh et al. [20], Love-type wave propagation in a corrugated piezoelectric layer over an isotropic elastic half-space is examined. Majhi et al. [21] established that the Love waves in a multilayer functionally graded piezoelectric system are affected by initial stress. The propagation of shear waves with a horizontal polarisation is examined by Sahu et al. [22] in a composite material with layers. The model under consideration has a functionally graded layer of piezoelectric material interceding between a corrugated layer of piezomagnetic material and a half-space. Functionally gradient material plates stimulated by plane pressure wavelets were the subject of research by Liu et al. [23] on elastic waves. In a piezoelectric layer with a half-infinite elastic layer, Liu et al. [24] examined the possibility of surface acoustic waves. Cao et al. [25] conducted a study on the behavior of Lamb waves in a plate made of functionally graded piezoelectric-piezomagnetic material. The material parameters were found to vary continuously along the thickness direction of the plate. Hemalatha et. al. [26] investigated the Rayleigh wave propagation in an elastic substrate and functionally graded piezoelectric layer. Sadab and Kundu [27] examined the characteristics of SH-wave propagation in a heterogeneous dry sandy half-space, which was bonded by a piezoelectric layer and abutting the vacuum.

Hemalatha et al. [28] delved into the propagation of Rayleigh waves in a structure comprising a functionally graded piezoelectric material (FGPM) layer over an elastic substrate. Singh [29,30] discussed the problem of Love waves in a layered medium bounded by an irregular bounded surface and also examined the propagation of SH waves by adopting Rayleigh's method of approximation. Singh et al. [31] studied the horizontally polarised shear wave (SH-wave) propagating in an elastic half-space having a corrugated and loosely connected common surface that has been initially stressed. An imperfect interface between a layer and two solids is studied by Lavrentyev and Rokhlin [32] using ultrasonic spectroscopy. Sahu et al. [33] encountered the problem of reflection and refraction of the incident plane waves at the loosely bonded interface of an isotropic elastic medium and a piezothermoelastic medium. Wang et al. [34] conducted research on the dispersion of an antiplane shear wave by a circular piezoelectric cylinder with an imperfect connection. Singh et al. [35] considered the propagation of torsional surface waves with

2

corrugated as well as loosely bonded boundary surfaces.

The WKB Approximation is a way to get the solution of a time-independent linear differential equation, it is named after the scientists who developed it, Wentzel-Kramers-Brillouin. In quantum physics, a semiclassical calculation usually involves rewriting the wavefunction as an exponential function, semiclassically expanding it, and then assuming that either the amplitude or phase is changing slowly. This method also makes the Froman and Froman [36] link between classical mechanics and quantum mechanics. The Love waves propagation in the functionally graded multilayer piezoelectric device is investigated by Liu and Wang [37] using the WKB approach. Jones [38] discovered the WKB approximation's uses in the computation of radio wave scattering from dense meteor trains. With the help of the WKB method, they were able to get approximate analytic solutions for Love waves. The comprehensive description of elastic wave propagation across layered, inhomogeneous media by Cerveny and Ravindra [39] is based on direct asymptotic expansion. Love wave behavior under initial stress is examined by Qian et al. [40] used the WKB technique in a functionally graded material layered non-piezoelectric half-space. Analysis of shear wave propagation in a piezoelectric structure comprised of an imperfectly bonded piezoelectric material layer was studied by Kumar et al. [41] using the WKB approach. In an FGPM layer coupled between a piezomagnetic plate and a pre-stressed piezoelectric half-space, Singhal et al. [42] used the WKB approach to explore the propagation of a Love-type wave.

Functionally graded materials (FGMs) have attracted intense research interest due to their ability to tailor material properties for specific applications, leading to advancements in everything from aircraft structures to medical implants. The widespread utilization of FGM in these applications serves as strong motivation for further exploration and investigation in this field.

This paper describes the propagation of polarized shear horizontal transverse waves in a layered composite structure consisting of a functionally graded magneto-electro-elastic layer imperfectly bonded to a piezoelectric semi-infinite medium, which is yet unaddressed for study as far as the known available literature. Previous studies primarily focused on investigating the behavior of horizontally polarized shear (SH) waves propagating through a FGPM layer that is imperfectly bonded to the functionally graded porous piezoelectric (FGPPM) half-space, employing the WKB method. The material coefficients of both the FGPM layer and the FGPPM half-space were assumed to exhibit functional gradedness, following a linear function of depth. In this work, the piezoelectric half-space and the magneto-electro-elastic layer's functionally graded material coefficients are both taken into consideration by the linear function of depth. Additionally, the solutions for layer and semi-infinite medium are found by reducing the partial differential equation to the ordinary differential equation using the fundamental variable-separable approach. An analytical method based on the WKB asymptotic method was used to solve an ordinary differential equation and to obtain a solution for both the layer and the semi-infinite medium. A dispersion relation is achieved for electrically open and electrically short scenarios in the form of a determinant. A specific model made up of a (BaTiO$_3$-CoFe$_2$O$_4$) magneto-electro-elastic material layer and a (BaTiO$_3$) piezoelectric semi-infinite medium has been used to determine the effects of the various parameters. Findings are represented using graphs with the help of Mathematica 7.

2. Problem formulation

Consider the magneto-electro-elastic structured layer depicted in Fig 1. It comprises a functionally graded piezoelectric semi-infinite medium and a functionally graded magneto-electro-elastic layer with a finite thickness *of* h and an imperfect bonding interface. The system's Cartesian coordinates are taken so that the x_1-axis is vertically downward and the x_2-axis is in the direction of shear horizontal transverse wave propagation along the interface between the functionally graded magneto-electro-elastic layer and functionally graded piezoelectric semi-infinite medium.
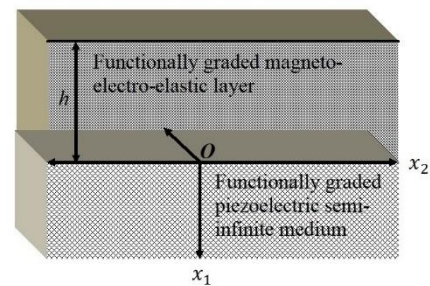

Figure 1: Geometry of the problem

The magneto-electro-elastic layer's field equations may be represented as

$$T_{ij,j} = \rho \ddot{u}_i$$
$$D_{i,i} = 0 \qquad (1)$$
$$B_{i,i} = 0$$

Here i, j =1,2,3, mass density is represented by ρ and D_i, u_i and B_i indicate the electric, mechanical, and magnetic displacements in the ith direction, correspondingly, the stress tensor is denoted by T_{ij}. The dot shows differentiation in

time, the comma shows differentiation in space, and the repeating index in the subscript shows summation.

The following is the relation between displacement and strain components is obtained from [41]:

$$S_{ij} = \tfrac{1}{2}\big(u_{i,j} + u_{j,i}\big). \tag{2}$$

Quasi-static approximation of the Maxwell equations yields:

$$\begin{aligned} E_i &= -\phi_{,i}, \\ H_i &= -\psi_{,i} \end{aligned} \tag{3}$$

Here, ϕ denotes the electrostatic potential and ψ denotes the magnetic potential.

For a transversely isotropic medium with x_3-axis as the symmetric axis and the poling axis of the magneto-electro-elastic material, the constitutive equations can be written in terms of components, which are obtained from [11].

$$\begin{aligned} T_{11} &= C_{11}S_{11} + C_{12}S_{22} + C_{13}S_{33} - e_{31}E_3 - h_{31}H_3 \\ T_{22} &= C_{12}S_{11} + C_{11}S_{22} + C_{13}S_{33} - e_{31}E_3 - h_{31}H_3 \\ T_{33} &= C_{13}S_{11} + C_{13}S_{22} + C_{33}S_{33} - e_{33}E_3 - h_{33}H_3 \\ T_{23} &= 2C_{44}S_{23} - e_{15}E_2 - h_{15}H_2 \\ T_{31} &= 2C_{44}S_{31} - e_{15}E_1 - h_{15}H_1 \\ T_{12} &= (C_{44} - C_{12})S_{12} \\ D_1 &= 2e_{15}S_{31} + \kappa_{11}E_1 + \beta_{11}H_1 \\ D_2 &= 2e_{15}S_{23} + \kappa_{11}E_2 + \beta_{11}H_2 \\ D_3 &= e_{31}S_{11} + e_{31}S_{22} + e_{33}S_{33} + \kappa_{33}E_3 + \beta_{33}H_3 \\ B_1 &= 2h_{15}S_{31} + \beta_{11}E_1 + \mu_{11}H_1 \\ B_2 &= 2h_{15}S_{23} + \beta_{11}E_2 + \mu_{11}H_2 \\ B_3 &= h_{31}S_{11} + h_{31}S_{22} + h_{31}S_{33} + \beta_{33}E_3 + \mu_{33}H_3 \end{aligned} \tag{4}$$

which x_1 is a function of the elastic constants C_{ij}, the dielectric constants κ_{ij} and the magnetic permittivity μ_{ij} $(i, j = 1,2,\ldots,6)$. Also e_{ij}, h_{ij} and β_{ij} are the piezoelectric, piezomagnetic, and electromagnetic constants functions of x_1 only. i.e., $C_{ij} = C_{ij}(x_1)$, $\kappa_{ij} = \kappa_{ij}(x_1)$, $\mu_{ij} = \mu_{ij}(x_1)$, $e_{ij} = e_{ij}(x_1)$, $h_{ij} = h_{ij}(x_1)$, $\beta_{ij} = \beta_{ij}(x_1)$.

Shear horizontal transverse wave propagation involves the shearing motion of waves within a material. Assuming the propagation of shear horizontal transverse waves in the x_2 direction, they induce displacements in the x_3 direction. The corresponding mechanical displacement, scalar electrical (ϕ), and magnetic potential function (ψ) components are given as follows:

$$\begin{aligned} u_1 &= 0 \\ u_2 &= 0 \\ u_3 &= u_3(x_1, x_2, t) \\ \phi &= \phi(x_1, x_2, t) \\ \psi &= \psi(x_1, x_2, t) \end{aligned} \tag{5}$$

and independent of x_3-coordinate.

The mechanical displacement is represented by u_{31}, whereas the electric and magnetic potential function is represented by ϕ_1 and ψ_1 in the region $-h < x_1 < 0$. Substituting condition (5) and Equations (4) into Equations (1), the equation of motion for shear horizontal transverse wave propagation is obtained as

$$T^{(1)}_{31,1} + T^{(1)}_{23,2} = \rho_1 \ddot{u}_{31} \tag{6}$$

$$D^{(1)}_{1,1} + D^{(1)}_{2,2} = 0 \tag{7}$$

$$B^{(1)}_{1,1} + B^{(1)}_{2,2} = 0 \tag{8}$$

The constitutive equations for a transversely isotropic magneto-electro-elastic material, with x3-axis being the symmetric axis of the material, are given by the following relationships between the stress, electric displacement, and magnetic displacement components, expressed in terms of mechanical and potential displacements:

$$\begin{aligned} T^{(1)}_{23} &= C^{(1)}_{44}(x_1)u_{31,2} + e^{(1)}_{15}(x_1)\phi_{1,2} \\ &\quad + h^{(1)}_{15}(x_1)\psi_{1,2}, \\ T^{(1)}_{31} &= C^{(1)}_{44}(x_1)u_{31,1} + e^{(1)}_{15}(x_1)\phi_{1,1} \\ &\quad + h^{(1)}_{15}(x_1)\psi_{1,1} \end{aligned} \tag{9}$$

$$\begin{aligned} D^{(1)}_1 &= e^{(1)}_{15}(x_1)u_{31,1} - \kappa^{(1)}_{11}(x_1)\phi_{1,1} \\ &\quad - \beta^{(1)}_{11}(x_1)\psi_{1,1}, \\ D^{(1)}_2 &= e^{(1)}_{15}(x_1)u_{31,2} - \kappa^{(1)}_{11}(x_1)\phi_{1,2} \\ &\quad - \beta^{(1)}_{11}(x_1)\psi_{1,2} \end{aligned} \tag{10}$$

$$\begin{aligned} B^{(1)}_1 &= h^{(1)}_{15}(x_1)u_{31,1} - \beta^{(1)}_{11}(x_1)\phi_{1,1} \\ &\quad - \mu^{(1)}_{11}(x_1)\psi_{1,1}, \\ B^{(1)}_2 &= h^{(1)}_{15}(x_1)u_{31,2} - \beta^{(1)}_{11}(x_1)(x_1)\phi_{1,2} \\ &\quad - \mu^{(1)}_{11}(x_1)\psi_{1,2} \end{aligned} \tag{11}$$

$$\rho_1 = \rho_1(x_1) \tag{12}$$

Equations (6), (7), (8), and (9) - (12) give us the field equations in the magneto-electro-elastic layer:

$$\begin{aligned} &C^{(1)}_{44}\big(u_{31,11} + u_{31,22}\big) + e^{(1)}_{15}\big(\phi_{1,11} + \phi_{1,22}\big) \\ &+ h^{(1)}_{15}\big(\psi_{1,11} + \psi_{1,22}\big) + C^{(1)\prime}_{44}{}^{u_{31,1}} + e^{(1)\prime}_{15}{}^{\phi_{1,1}} \\ &+ h^{(1)\prime}_{15}\psi_{1,1} = \rho_1 \ddot{u}_{31} \end{aligned} \tag{13}$$

$$\begin{aligned} &e^{(1)}_{15}\big(u_{31,11} + u_{31,22}\big) - \kappa^{(1)}_{11}\big(\phi_{1,11} + \\ &\phi_{1,22}\big) - \beta^{(1)}_{11}\big(\psi_{1,11} + \psi_{1,22}\big) + \\ &e^{(1)\prime}_{15}u_{31,1} - \kappa^{(1)\prime}_{11}\phi_{1,1} - \beta^{(1)\prime}_{11}\psi_{1,1} = 0 \end{aligned} \tag{14}$$

$$h_{15}^{(1)}(u_{31,11} + u_{31,22}) - \beta_{11}^{(1)}(\phi_{1,11} + \phi_{1,22}) - \mu_{11}^{(1)}(\psi_{1,11} + \psi_{1,22}) + h_{15}^{(1)\prime}u_{31,1} - \beta_{11}^{(1)\prime}\phi_{1,1} - \mu_{11}^{(1)\prime}\psi_{1,1} = 0 \tag{15}$$

where " ′ " denote the differentiation with respect to x_1.

For propagation of shear horizontal transverse waves in a semi-infinite medium, the solution to the equation of motion is as follows:

$$T_{31,1}^{(2)} + T_{23,2}^{(2)} = \rho_2 \ddot{u}_{32} \tag{16}$$

$$D_{1,1}^{(2)} + D_{2,2}^{(2)} = 0 \tag{17}$$

$$B_{1,1}^{(2)} + B_{2,2}^{(2)} = 0 \tag{18}$$

The stress, electric and magnetic displacement components are characterized as follows in terms of mechanical and potential displacement:

$$T_{31}^{(2)} = C_{44}^{(2)}(x_1)u_{32,1} + e_{15}^{(2)}(x_1)\phi_{2,1},$$
$$T_{32}^{(2)} = C_{44}^{(2)}(x_1)u_{32,2} + e_{15}^{(2)}(x_1)\phi_{2,2} \tag{19}$$

$$D_1^{(2)} = e_{15}^{(2)}(x_1)u_{32,1} - \kappa_{11}^{(2)}(x_1)\phi_{2,1},$$
$$D_2^{(2)} = e_{15}^{(2)}(x_1)u_{32,2} - \kappa_{11}^{(2)}(x_1)\phi_{2,2} \tag{20}$$

$$B_1^{(2)} = -\mu_{11}^{(2)}(x_1)\psi_{2,1},$$
$$B_1^{(2)} = -\mu_{11}^{(2)}(x_1)\psi_{2,2} \tag{21}$$

$$\rho_2 = \rho_2(x_1) \tag{22}$$

Equations (16)-(18) and (19)-(22) give us the field equations for the piezoelectric layer:

$$C_{44}^{(2)}(u_{32,11} + u_{32,22}) + e_{15}^{(2)}(\phi_{2,11} + \phi_{2,22}) + C_{44}^{(2)\prime}u_{32,1} + e_{15}^{(2)\prime}\phi_{2,1} = \rho_2 \ddot{u}_{32} \tag{23}$$

$$e_{15}^{(2)}(u_{32,11} + u_{32,22}) - \kappa_{11}^{(2)}(\phi_{2,11} + \phi_{2,22}) + e_{15}^{(2)\prime}u_{32,1} - \kappa_{11}^{(2)\prime}\phi_{2,1} = 0 \tag{24}$$

$$\mu_{11}^{(2)}(\psi_{2,11} + \psi_{2,22}) + \mu_{11}^{(2)\prime}\psi_{2,1} = 0 \tag{25}$$

where " ′ " denote the differentiation with respect to x_1.

Air's dielectric constant κ_0 and μ_0 varies substantially from the dielectric constant of piezoelectric and magneto-electro-elastic materials. As a result, the magneto-electro-elastic layer's upper surface is often exposed to air. Therefore, electric and magnetic potential function ϕ_0 and ψ_0 may be considered a vacuum for air in the region $x_1 < -h$.

$$\phi_{0,11} + \phi_{0,22} = 0$$
$$\psi_{0,11} + \psi_{0,22} = 0 \tag{26}$$

The electric and magnetic displacement components of a vacuum are described as follows

$$D_1^{(0)} = -\kappa_0\phi_{0,1},$$
$$B_1^{(0)} = -\mu_0\psi_{0,1} \tag{27}$$

3. Problem formulation

3.1. Solution of the functionally graded magneto-electro-elastic layer

Equations (13), (14) and (15) can be solved by assuming the following solution:

$$\{u_{31}, \phi_1, \psi_1\}(x_1, x_2, t) = \{U_{31}, \Phi_1, \Psi_1\}(x_1)e^{ik(x_2 - ct)} \tag{28}$$

denoting wave number as $k\left(= \frac{2\pi}{\lambda}\right)$ and wavelength as λ, as well as wave propagation phase velocity as c and $i = \sqrt{-1}$.

By using equation (28), equation (13), (14) and (15) reduces to

$$C_{44}^{(1)}(x_1)U_{31}'' + C_{44}^{(1)\prime}(x_1)U_{31}' + [\rho_1(x_1)c^2 - C_{44}^{(1)}(x_1)]k^2 U_{31} + e_{15}^{(1)}(x_1)\Phi_1'' + e_{15}^{(1)\prime}(x_1)\Phi_1' + k^2 e_{15}^{(1)}(x_1) + h_{15}^{(1)}(x_1)\Psi_1'' + h_{15}^{(1)\prime}(x_1)\Psi_1' - k^2 h_{15}^{(1)}(x_1)\Psi_1 = 0 \tag{29}$$

$$e_{15}^{(1)}(x_1)U_{31}'' + e_{15}^{(1)\prime(x_1)U_{31}'} - k^2 e_{15}^{(1)}(x_1)U_{31} - \kappa_{11}^{(1)}(x_1)\Phi_1'' - \kappa_{11}^{(1)\prime}(x_1)\Phi_1' + k^2 \kappa_{11}^{(1)}(x_1)\Phi_1 - \beta_{11}^{(1)}(x_1)\Psi_1'' - \beta_{11}^{(1)\prime}(x_1)\Psi_1' + k^2 \beta_{11}^{(1)}(x_1)\Psi_1 = 0 \tag{30}$$

$$h_{15}^{(1)}(x_1)U_{31}'' + h_{15}^{(1)\prime}(x_1)U_{31}' - k^2 h_{15}^{(1)}(x_1)U_{31} - \beta_{11}^{(1)}(x_1)\Phi_1'' - \beta_{11}^{(1)\prime}(x_1)\Phi_1' + k^2 \beta_{11}^{(1)}(x_1)\Phi_1 - \mu_{11}^{(1)}(x_1)\Psi_1'' - \mu_{11}^{(1)\prime}(x_1)\Psi_1' + k^2 \mu_{11}^{(1)}(x_1)\Psi_1 = 0 \tag{31}$$

The functionally graded magneto-electro-elastic layer has linear function distributions in the direction of x_1 axis because functionally gradedness enhances the magneto-electro-elastic material layer's properties. As a consequence, the functionally graded magneto-electro-elastic layer's material attributes are classified as

$$C_{44}^{(1)}(x_1) = C_{44}^{10}[1 + \alpha_1(h + x_1)]$$
$$e_{15}^{(1)}(x_1) = e_{15}^{10}[1 + \alpha_1(h + x_1)] \tag{32}$$

5

$$h_{15}^{(1)}(x_1) = h_{15}^{10}[1 + \alpha_1(h + x_1)]$$

$$\kappa_{11}^{(1)}(x_1) = \kappa_{11}^{10}[1 + \alpha_1(h + x_1)]$$

$$\beta_{11}^{(1)}(x_1) = \beta_{11}^{10}[1 + \alpha_1(h + x_1)]$$

$$\mu_{11}^{(1)}(x_1) = \mu_{11}^{10}[1 + \alpha_1(h + x_1)]$$

$$\rho_1(x_1) = \rho_{10}[1 + \alpha_1(h + x_1)]$$

where C_{44}^{10}, e_{15}^{10}, h_{15}^{10}, κ_{11}^{10}, β_{11}^{10}, μ_{11}^{10} and ρ_{10} are the homogenous values of $C_{44}^{(1)}$, $e_{15}^{(1)}$, $h_{15}^{(1)}$, $\kappa_{11}^{(1)}$, $\beta_{11}^{(1)}$, $\mu_{11}^{(1)}$ and ρ_1 at $x_2 = -h$. The inverse of the length of the gradient material parameter is represented by the α_1.

Substituting equation (32) in equation (29), (30) and (31), we get

$$
\begin{aligned}
&C_{44}^{10}[1 + \alpha_1(h + x_1)]U_{31}'' + C_{44}^{10}\alpha_1 U_{31}' + \\
&[\rho_{10}[1 + \alpha_1(h + x_1)]c^2 - C_{44}^{10}[1 + \alpha_1(h + \\
&x_1)]]k^2 U_{31} + e_{15}^{10}[1 + \alpha_1(h + x_1)]\Phi_1'' + \\
&e_{15}^{10}\alpha_1 \Phi_1' - k^2 e_{15}^{10}[1 + \alpha_1(h + x_1)]\Phi_1 + \\
&h_{15}^{10}[1 + \alpha_1(h + x_1)]\Psi_1'' + h_{15}^{10}\alpha_1 \Psi_1' - \\
&k^2 h_{15}^{10}[1 + \alpha_1(h + x_1)]\Psi_1 = 0
\end{aligned}
\tag{33}
$$

$$
\begin{aligned}
&e_{15}^{10}[1 + \alpha_1(h + x_1)]U_{31}'' + e_{15}^{10}\alpha_1 U_{31}' - \\
&k^2 e_{15}^{10}[1 + \alpha_1(h + x_1)]U_{31} - \kappa_{11}^{10}[1 + \\
&\alpha_1(h + x_1)]\Phi_1'' - \kappa_{11}^{10}\alpha_1 \Phi_1' + k^2 \kappa_{11}^{10}[1 + \\
&\alpha_1(h + x_1)]\Phi_1 - \beta_{11}^{10}[1 + \alpha_1(h + \\
&x_1)]\Psi_1'' - \beta_{11}^{10}\alpha_1 \Psi_1' + k^2 \beta_{11}^{10}[1 + \alpha_1(h + \\
&x_1)]\Psi_1 = 0
\end{aligned}
\tag{34}
$$

$$
\begin{aligned}
&h_{15}^{10}[1 + \alpha_1(h + x_1)]U_{31}'' + h_{15}^{10}\alpha_1 U_{31}' - \\
&k^2 h_{15}^{10}[1 + \alpha_1(h + x_1)]U_{31} - \beta_{11}^{10}[1 + \\
&\alpha_1(h + x_1)]\Phi_1'' - \beta_{11}^{10}\alpha_1 \Phi_1' + k^2 \beta_{11}^{10}[1 + \\
&\alpha_1(h + x_1)]\Phi_1 - \mu_{11}^{10}[1 + \alpha_1(h + \\
&x_1)]\Psi_1'' - \mu_{11}^{10}\alpha_1 \Psi_1' + k^2 \mu_{11}^{10}[1 + \alpha_1(h + \\
&x_1)]\Psi_1 = 0
\end{aligned}
\tag{35}
$$

Rearranging Equations (33), (34), and (35), and let

$a_1(x_1) = [1 + \alpha_1(h + x_1)]$, $a_2 = \frac{e_{15}^{10}\mu_{11}^{10} - \beta_{11}^{10}h_{15}^{10}}{\mu_{11}^{10}\kappa_{11}^{10} - (\beta_{11}^{10})^2}$,

$a_3 = \frac{h_{15}^{10}\kappa_{11}^{10} - \beta_{11}^{10}e_{15}^{10}}{\mu_{11}^{10}\kappa_{11}^{10} - (\beta_{11}^{10})^2}$ and $A^0 = C_{44}^{10} + e_{15}^{10}a_2 + h_{15}^{10}a_3$

$$U_{31}'' + \frac{\alpha_1}{a_1}U_{31}' + k^2\left(\frac{\rho_{10}c^2}{A^0} - 1\right)U_{31} = 0 \tag{36}$$

$$\Phi_1'' + \frac{\alpha_1}{a_1}\Phi_1' - k^2\Phi_1 = a_2\left(U_{31}'' + \frac{\alpha_1}{a_1}U_{31}' - k^2 U_{31}\right) \tag{37}$$

$$\Psi_1'' + \frac{\alpha_1}{a_1}\Psi_1' - k^2\Psi_1 = a_3\left(U_{31}'' + \frac{\alpha_1}{a_1}U_{31}' - k^2 U_{31}\right) \tag{38}$$

This is a second-order differential equation with variable coefficients. The asymptotic solutions to these equations can be determined

using the WKB approach, which is a high-frequency and shortwave technique with a wave number of $k \gg 1$. Equation (36) may be approximated asymptotically using the WKB approach by following this strategy. Using the phase integral approach, we may propose the following transformation.

$$U_{31}(x_1) = e^{\int \lambda(x_1)dx_1} \tag{39}$$

Equation (36) can be converted into the following form using equation (39)

$$\lambda^2 + \lambda' + \frac{\alpha_1}{a_1}\lambda + \left(\frac{\rho_{10}c^2}{A^0} - 1\right)k^2 = 0 \tag{40}$$

For which the asymptotic series expansion in terms of the inverse power of k may be found as follows

$$\lambda(x_1) = \lambda_0(x_1)k + \lambda_1(x_1) + \frac{\lambda_2(x_1)}{k} + \dots \tag{41}$$

We can create an infinite number of equations by replacing equation (41) with equation (40), comparing the coefficients of k, and then setting them equal to zero.

$$
\begin{aligned}
&\lambda_0^2 + \left(\frac{\rho_{10}c^2}{A^0} - 1\right) = 0 \\
&2\lambda_0\lambda_1 + \lambda_0' + \frac{\alpha_1}{a_1}\lambda_0 = 0 \\
&\lambda_1^2 + 2\lambda_0\lambda_2 + \lambda_1' + \frac{\alpha_1}{a_1}\lambda_1 = 0
\end{aligned}
\tag{42}
$$

$$\vdots$$

The following are the solutions to the preceding system of equations

$$\lambda_0^{(1)} = i\sqrt{\left(\frac{\rho_{10}c^2}{A^0} - 1\right)}, \lambda_0^{(2)} = -i\sqrt{\left(\frac{\rho_{10}c^2}{A^0} - 1\right)}$$

$$\lambda_1^{(1)} = \lambda_1^{(2)} = -\frac{\alpha_1}{2a_1}$$

$$\lambda_2^{(1)} = \frac{i\alpha_1^2}{8a_1^2}\sqrt{\left(\frac{A^0}{\rho_{10}c^2 - A^0}\right)}, \tag{43}$$

$$\lambda_2^{(2)} = -\frac{i\alpha_1^2}{8a_1^2}\sqrt{\left(\frac{A^0}{\rho_{10}c^2 - A^0}\right)}$$

$$\vdots$$

Equation (43) solutions can be swapped into equation (41).

$$
\begin{aligned}
\lambda^{(1)} = &ik\sqrt{\left(\frac{\rho_{10}c^2}{A^0} - 1\right)} - \frac{\alpha_1}{2a_1} \\
&+ \frac{i\alpha_1^2}{8ka_1^2}\sqrt{\left(\frac{A^0}{\rho_{10}c^2 - A^0}\right)}\dots
\end{aligned}
\tag{44}
$$

$$\lambda^{(2)} = -ik\sqrt{\left(\frac{\rho_{10}c^2}{A^0} - 1\right)} - \frac{\alpha_1}{2a_1}$$
$$-\frac{i\alpha_1^2}{8ka_1{}^2}\sqrt{\left(\frac{A^0}{\rho_{10}c^2 - A^0}\right)} \dots,$$

Using equation (44), equation (39) can be written as

$$U_{31}(x_1) = \frac{D_1 e^{is_1(x_1)} + D_2 e^{-is_1(x_1)}}{\sqrt{1 + \alpha_1(h + x_1)}} \qquad (45)$$

where D_1, D_2 are undetermined constants and

$$s_1(x_1) = kx_1\sqrt{\frac{\rho_{10}c^2}{A^0} - 1} - \frac{\alpha_1}{8ka_1}\sqrt{\frac{A^0}{\rho_{10}c^2 - A^0}}$$

With the aid equation (45), equation (39) yields

$$u_{31}(x_1, x_2, t) = \frac{D_1 e^{is_1(x_1)} + D_2 e^{-is_1(x_1)}}{\sqrt{1 + \alpha_1(h + x_1)}} e^{ik(x_2 - ct)} \qquad (46)$$

Using the same asymptotic method and substituting equation (46) for equations (37) and (38), the entire solution of $\Phi_1(x_1, x_2, t)$ and $\Psi_1(x_1, x_2, t)$ can be represented as

$$\phi_1(x_1, x_2, t) = \frac{D_3 e^{s_2(x_1)} + D_4 e^{-s_2(x_1)}}{\sqrt{1 + \alpha_1(h + x_1)}} e^{ik(x_2 - ct)} + a_2 u_{31}(x_1, x_2, t) \qquad (47)$$

$$\psi_1(x_1, x_2, t) = \frac{D_5 e^{s_2(x_1)} + D_6 e^{-s_2(x_1)}}{\sqrt{1 + \alpha_1(h + x_1)}} e^{ik(x_2 - ct)} + a_3 u_{31}(x_1, x_2, t) \qquad (48)$$

where D_3, D_4, D_5 and D_6 are undetermined constants and
$$s_2(x_1) = kx_1 + \frac{\alpha_1}{8ka_1}$$

3.2. Solution for functionally graded piezoelectric semi-infinite medium

Equations (23), (24) and (25) can be solved by assuming the following solution:

$$\{u_{32}, \phi_2, \psi_2\}(x_1, x_2, t) = \{U_{32}, \Phi_2, \Psi_2\}(x_1)e^{ik(x_2 - ct)} \qquad (49)$$

By using equation (49), equation (23), (24) and (25) reduces to

$$C_{44}^{(2)}(x_1)U_{32}'' + C_{44}^{(2)'}(x_1)U_{32}' + [\rho_2(x_1)c^2 - C_{44}^{(2)}(x_1)]k^2 U_{32} + e_{15}^{(2)}(x_1)\Phi_2'' + e_{15}^{(2)'}(x_1)\Phi_2' - k^2 e_{15}^{(2)}(x_1)\Phi_2 = 0 \qquad (50)$$

$$e_{15}^{(2)}(x_1)U_{32}'' + e_{15}^{(2)'}(x_1)U_{32}' - k^2 e_{15}^{(2)}(x_1)U_{32} - \kappa_{11}^{(2)}(x_1)\Phi_2'' - \kappa_{11}^{(2)'}(x_1)\Phi_2' + k^2\kappa_{11}^{(2)}(x_1)\Phi_2 = 0 \qquad (51)$$

$$\mu_{11}^{(2)}(x_1)\Psi_2'' + \mu_{11}^{(2)'}(x_1)\Psi_2' - k^2\mu_{11}^{(2)}(x_1)\Psi_2 = 0 \qquad (52)$$

The functionally graded piezoelectric semi-infinite medium has linear function distributions in the direction of x_1 axis because functionally gradedness enhances the piezoelectric material properties. As a consequence, the functionally graded piezoelectric semi-infinite medium material attributes are classified as

$$C_{44}^{(2)}(x_1) = C_{44}^{20}[1 + \alpha_2 x_1]$$
$$e_{15}^{(2)}(x_1) = e_{15}^{20}[1 + \alpha_2 x_1]$$
$$\kappa_{11}^{(2)}(x_1) = \kappa_{11}^{20}[1 + \alpha_2 x_1]$$
$$\mu_{11}^{(2)}(x_1) = \mu_{11}^{20}[1 + \alpha_2 x_1] \qquad (53)$$
$$\rho_2^{(2)}(x_1) = \rho_{20}[1 + \alpha_2 x_1]$$

where C_{44}^{20}, e_{15}^{20}, κ_{11}^{20}, μ_{11}^{20} and ρ_{20} are the homogenous values of $C_{44}^{(2)}$, $e_{15}^{(2)}$, $\kappa_{11}^{(2)}$, $\mu_{11}^{(2)}$ and $\rho_2^{(2)}$. The inverse of the length of the gradient material parameter is represented by the α_2.

Substituting equation (53) in equation (50), (51) and (52) and letting and $B^0 = C_{44}^{20} + \frac{(e_{15}^{20})^2}{\kappa_{11}^{20}}$ and $b_1(x_1) = [1 + \alpha_2 x_1]$ we get

$$U_{32}'' + \frac{\alpha_2}{b_1}U_{32}' + k^2\left(\frac{\rho_{20}c^2}{B^0} - 1\right)U_{32} = 0 \qquad (54)$$

$$\Phi_2'' + \frac{\alpha_2}{b_1}\Phi_2' - k^2\Phi_2 = \frac{e_{15}^1}{\kappa_{11}^1}\left(U_{32}'' + \frac{\alpha_2}{b_1}U_{32}' - k^2 U_{32}\right) \qquad (55)$$

$$\Psi_2'' + \frac{\alpha_2}{b_1}\Psi_2' - k^2\Psi_2 = 0 \qquad (56)$$

The same asymptotic WKB method that is used to solve for a functionally graded magneto-electro-elastic layer can also be used to solve expression (54) for a functionally graded piezoelectric semi-infinite medium.

We're looking for a solution for mechanical displacement and electric potential expression in a semi-infinite medium where mechanical displacement and electric potential diminish as depth increases which means as $x_1 \to \infty$, $u_{32} \to 0$, $\phi_2 \to 0$. The solution to this problem is thus an approximation, which is

$$u_{32}(x_1, x_2, t) = \frac{D_7 e^{-is_3(x_1)}}{\sqrt{1 + \alpha_2 x_1}} e^{ik(x_2 - ct)} \qquad (57)$$

where D_7 is undetermined constants and

7

$$s_3(x_1) = kx_1\sqrt{\frac{\rho_{20}c^2}{B^0} - 1} - \frac{\alpha_2}{8kb_1}\sqrt{\frac{B^0}{\rho_{20}c^2 - B^0}}$$

Using the same asymptotic method and substituting equation (57) for equation (55), the entire solution of $\Phi_2(x_1, x_2, t)$ can be represented as

$$\phi_2(x_1, x_2, t) = \frac{D_8 e^{-s_4(x_1)}}{\sqrt{1 + \alpha_2 x_1}} e^{ik(x_2 - ct)} \qquad (58)$$
$$+ \frac{e_{15}^1}{\kappa_{11}^1} u_{32}(x_1, x_2, t)$$

The entire solution of $\Psi_2(x_1, x_2, t)$ can be represented as

$$\psi_2(x_1, x_2, t) = \frac{D_9 e^{-s_4(x_1)}}{\sqrt{1 + \alpha_2 x_1}} e^{ik(x_2 - ct)} \qquad (59)$$

where D_8 and D_9 is undetermined constants and $s_4(x_1) = kx_1 + \frac{\alpha_2}{8kb_1}$

3.3. Solution for the vacuum

The solution to equation (26) is obtained by, assuming that the electric and magnetic potential function ϕ_0 and ψ_0 diminishes as $x_1 \to -\infty$ which results in

$$\phi_0(x_1, x_2, t) = D_{10} e^{kx_1} e^{ik(x_2 - ct)}$$
$$\psi_0(x_1, x_2, t) = D_{11} e^{kx_1} e^{ik(x_2 - ct)} \qquad (60)$$

where D_{10} and D_{11} is undetermined constants.

4. Boundary Conditions

In this problem, both the functionally graded magneto-electro-elastic layer and the piezoelectric semi-infinite medium have a mechanically imperfect interface. Only the upper boundary is considered electrically open and short-case. At the interface, the electrical displacement and scalar potential function are considered continuous. These conditions are illustrated mathematically below.

1) The mechanical traction-free condition at the free surface $x_1 = -h$ of the functionally graded magneto-electro-elastic layer is given by

    i. $T_{31}^{(1)} = 0$

$$\Rightarrow [1 + \alpha_1(h + x_1)][C_{44}^{10} u_{31,1} + \qquad (61)$$
$$e_{15}^{10}\Phi_{1,1} + h_{15}^{10}\Psi_{1,1}] = 0$$

2) The electrical boundary condition at $x_1 = -h$ are

  a) Electrically open case

    i. $\phi_1 = \phi_0$

    ii. $D_1^{(1)} = D_1^{(0)}$

$$\Rightarrow [1 + \alpha_1(h + x_1)][e_{15}^{10} u_{31,1} - \qquad (62)$$
$$\kappa_{11}^{10}\Phi_{1,1} - \beta_{11}^{10}\Psi_{1,1}] = \kappa_0\phi_{0,1}$$

    iii. $\psi_1 = \psi_0$

    iv. $B_1^{(1)} = B_1^{(0)}$

$$\Rightarrow [1 + \alpha_1(h + x_1)][h_{15}^{10} u_{31,1} -$$
$$\beta_{11}^{10}\Phi_{1,1} - \mu_{11}^{10}\Psi_{1,1}] = \mu_0\Psi_{0,1}$$

  b) Electrically short case

    i. $\phi_1 = 0$

    ii. $\psi_1 = 0$ (63)

3) It is assumed that the interface of functionally graded magneto-electro-elastic layer and functionally graded piezoelectric semi-infinite medium is damaged mechanically. For the imperfect interfacial bonding, the stresses and electric displacements are continuous at $x_1 = 0$

    i. $T_{31}^{(1)} = T_{31}^{(2)}$

$$\Rightarrow [1 + \alpha_1(h + x_1)][C_{44}^{10} u_{31,1} +$$
$$e_{15}^{10}\Phi_{1,1} + h_{15}^{10}\Psi_{1,1}] =$$
$$[1 + \alpha_2 x_1][C_{44}^{20} u_{32,1} + e_{15}^{20}\Phi_{2,1}]$$

    ii. $T_{31}^{(2)} = K[u_{31} - u_{32}]$

$$\Rightarrow [1 + \alpha_2 x_1][C_{44}^{20} u_{32,1} + e_{15}^{20}\Phi_{2,1}] =$$
$$K[u_{31} - u_{32}]$$

    iii. $\phi_1 = \phi_2$

    iv. $\psi_1 = \psi_2$

    v. $D_1^{(1)} = D_1^{(2)}$ (64)

$$\Rightarrow [1 + \alpha_1(h + x_1)][e_{15}^{10} u_{31,1} -$$
$$\kappa_{11}^{10}\Phi_{1,1} - \beta_{11}^{10}\Psi_{1,1}] =$$
$$[1 + \alpha_2 x_1][e_{15}^{20} u_{32,1} - \kappa_{11}^{20}\Phi_{2,1}]$$

    vi. $B_1^{(1)} = B_1^{(2)}$

$$\Rightarrow [1 + \alpha_1(h + x_1)][h_{15}^{10} u_{31,1} -$$
$$\beta_{11}^{10}\Phi_{1,1} - \mu_{11}^{10}\Psi_{1,1}] =$$
$$-[1 + \alpha_2 x_1][\mu_{11}^{20}\Psi_{2,1}]$$

where K is the mechanical interfacial imperfection bonding parameter which are uniform and non-negative. Obviously, if $K \to 0$, the interface of the layer and semi-infinite medium is perfectly bonded and conducting. Otherwise, it is mechanically imperfect.

5. Dispersion relations

Using Equations (46), (47), (48), (57), (58), (59), and (60) into boundary conditions (61) to (64) homogeneous equations for the unknown variables D_1 to D_{11} are obtained.

8

$$A^0 \left(\frac{-\alpha_1}{2} + i f_1\right) e^{i p_1} D_1 - A^0 \left(\frac{\alpha_1}{2} + i f_1\right) e^{-i p_1} D_2 + e_{15}^{10} \left(\frac{-\alpha_1}{2} + f_2\right) e^{p_2} D_3 - e_{15}^{10} \left(\frac{\alpha_1}{2} + f_2\right) e^{-p_2} D_4 + h_{15}^{10} (\frac{-\alpha_1}{2} + f_2) e^{p_2} D_5 - h_{15}^{10} (\frac{\alpha_1}{2} + f_2) e^{-p_2} D_6 = 0 \tag{65}$$

$$a_2 e^{i p_1} D_1 + a_2 e^{-i p_1} D_2 + e^{p_2} D_3 + e^{-p_2} D_4 - e^{-kh} D_{10} = 0 \tag{66}$$

$$m^0 \left(\frac{-\alpha_1}{2} + i f_1\right) e^{i p_1} D_1 - m^0 \left(\frac{\alpha_1}{2} + i f_1\right) e^{-i p_1} D_2 - \kappa_{11}^{10} \left(\frac{-\alpha_1}{2} + f_2\right) e^{p_2} D_3 + \kappa_{11}^{10} \left(\frac{\alpha_1}{2} + f_2\right) e^{-p_2} D_4 - \beta_{11}^{10} \left(\frac{-\alpha_1}{2} + f_2\right) e^{p_2} D_5 + \beta_{11}^{10} \left(\frac{\alpha_1}{2} + f_2\right) e^{-p_2} D_6 + \kappa_0 k e^{-kh} D_{10} \tag{67}$$

$$a_3 e^{i p_1} D_1 + a_3 e^{-i p_1} D_2 + e^{p_2} D_5 + e^{-p_2} D_6 - e^{-kh} D_{11} = 0 \tag{68}$$

$$l^0 \left(\frac{-\alpha_1}{2} + i f_1\right) e^{i p_1} D_1 - l^0 \left(\frac{\alpha_1}{2} + i f_1\right) e^{-i p_1} D_2 - \beta_{11}^{10} \left(\frac{-\alpha_1}{2} + f_2\right) e^{p_2} D_3 + \beta_{11}^{10} \left(\frac{\alpha_1}{2} + f_2\right) e^{-p_2} D_4 - \mu_{11}^{10} \left(\frac{-\alpha_1}{2} + f_2\right) e^{p_2} D_5 + \mu_{11}^{10} (\frac{\alpha_1}{2} + f_2) e^{-p_2} D_6 + \mu_0 k e^{-kh} D_{11} = 0 \tag{69}$$

$$a_2 e^{i p_1} D_1 + a_2 e^{-i p_1} D_2 + e^{p_2} D_3 + e^{-p_2} D_4 = 0 \tag{70}$$

$$a_3 e^{i p_1} D_1 + a_3 e^{-i p_1} D_2 + e^{p_2} D_5 + e^{-p_2} D_6 = 0 \tag{71}$$

$$A^0 d_1 \left(\frac{-\alpha_1}{2d_1} + i\sqrt{d_1} f_3\right) e^{i p_3} D_1 - A^0 d_1 \left(\frac{\alpha_1}{2d_1} + i\sqrt{d_1} f_3\right) e^{-i p_3} D_2 + e_{15}^{10} d_1 \left(\frac{-\alpha_1}{2d_1} + \sqrt{d_1} f_4\right) e^{p_4} D_3 - e_{15}^{10} d_1 \left(\frac{\alpha_1}{2d_1} + \sqrt{d_1} f_4\right) e^{-p_4} D_4 + h_{15}^{10} d_1 \left(\frac{-\alpha_1}{2d_1} + \sqrt{d_1} f_4\right) e^{p_4} D_5 - h_{15}^{10} d_1 \left(\frac{\alpha_1}{2d_1} + \sqrt{d_1} f_4\right) e^{-p_4} D_6 - B^0 (\frac{\alpha_2}{2} + i f_5) e^{-i p_5} D_7 + e_{15}^{20} (\frac{\alpha_2}{2} + f_6) e^{-p_6} D_8 = 0 \tag{72}$$

$$\frac{-K}{\sqrt{d_1}} e^{i p_3} D_1 - \frac{K}{\sqrt{d_1}} e^{-i p_3} D_2 + (-B^0 (\frac{\alpha_2}{2} + i f_5) + K) e^{-i p_5} D_7 - e_{15}^{20} (\frac{\alpha_2}{2} + f_6) e^{-p_6} D_8 = 0 \tag{73}$$

$$\frac{a_2}{\sqrt{d_1}} e^{i p_3} D_1 + \frac{a_2}{\sqrt{d_1}} e^{-i p_3} D_2 + \frac{1}{\sqrt{d_1}} e^{p_4} D_3 + \frac{1}{\sqrt{d_1}} e^{-p_4} D_4 - \frac{e_{15}^{20}}{\kappa_{11}^{20}} e^{-i p_5} D_7 - e^{-p_6} D_8 = 0 \tag{74}$$

$$\frac{a_3}{\sqrt{d_1}} e^{i p_3} D_1 + \frac{a_3}{\sqrt{d_1}} e^{-i p_3} D_2 + \frac{1}{\sqrt{d_1}} e^{p_4} D_5 + \frac{1}{\sqrt{d_1}} e^{-p_4} D_6 - e^{-p_6} D_9 = 0 \tag{75}$$

$$m^0 d_1 \left(\frac{-\alpha_1}{2d_1} + i\sqrt{d_1} f_3\right) e^{i p_3} D_1 - m^0 d_1 \left(\frac{\alpha_1}{2d_1} + i\sqrt{d_1} f_3\right) e^{-i p_3} D_2 - \kappa_{11}^{10} d_1 \left(\frac{-\alpha_1}{2d_1} + \sqrt{d_1} f_4\right) e^{p_4} D_3 + \kappa_{11}^{10} d_1 \left(\frac{\alpha_1}{2d_1} + \sqrt{d_1} f_4\right) e^{-p_4} D_4 - \beta_{11}^{10} \left(\frac{-\alpha_1}{2} + f_2\right) e^{p_2} D_5 + \beta_{11}^{10} \left(\frac{\alpha_1}{2} + f_2\right) e^{-p_2} D_6 - \kappa_{11}^{20} (\frac{\alpha_2}{2} + f_6) e^{-p_6} D_8 = 0 \tag{76}$$

$$l^0 d_1 \left(\frac{-\alpha_1}{2d_1} + i\sqrt{d_1} f_3\right) e^{i p_3} D_1 - l^0 d_1 \left(\frac{\alpha_1}{2d_1} + i\sqrt{d_1} f_3\right) e^{-i p_3} D_2 - \beta_{11}^{10} d_1 \left(\frac{-\alpha_1}{2d_1} + \sqrt{d_1} f_4\right) e^{p_4} D_3 + \beta_{11}^{10} d_1 \left(\frac{\alpha_1}{2d_1} + \sqrt{d_1} f_4\right) e^{-p_4} D_4 - \mu_{11}^{10} d_1 \left(\frac{-\alpha_1}{2d_1} + \sqrt{d_1} f_4\right) e^{p_4} D_5 + \mu_{11}^{10} d_1 \left(\frac{\alpha_1}{2d_1} + \sqrt{d_1} f_4\right) e^{-p_4} D_6 + \mu_{11}^{20} (\frac{\alpha_2}{2} + f_6) e^{-p_6} D_9 = 0 \tag{77}$$

where $f_1, f_2, f_3, f_4, f_5, f_6, p_1, p_2, p_3, p_4, p_5, p_6, d_1 \, l^0$ and m^0 are defined in Appendix A.

5.1. Electrically open case

The dispersion relation of the shear horizontal transverse wave for a functionally graded magneto-electro-elastic layer covering a piezoelectric semi-infinite medium subjected to the boundary condition specified in section 4 is extracted in eleventh-order determinant form by eliminating $D_1 - D_{11}$ from the following Equations (65) to (69) and (71) to (77).

$$|r_{ij}|_{11 \times 11} = 0, \quad \forall i,j = 1,2,..11 \tag{78}$$

where r_{ij} defined in Appendix B.

5.2. Electrically short case

Excluding $D_1 - D_9$ and from the following Equations (65), (70) to (77) we arrive at the ninth-order determinant form of the dispersion relation for the shear horizontal functionally graded magneto-electro-elastic layer covering a piezoelectric semi-infinite medium subject to the boundary condition discussed in section 4.

$$|t_{ij}|_{9 \times 9} = 0, \quad \forall i,j = 1,2,..,9 \tag{79}$$

Here t_{ij} defined in Appendix C.

6. Special cases

Case 1 When $x_1 = 0$, $x_2 = -h$, and $K \to \infty$ (i.e., the layer and semi-infinite medium have a perfect bonding interface), the dispersion relations for shear wave propagation in a functionally graded magneto-electro-elastic layer of uniform thickness overlying a functionally graded piezoelectric semi-infinite medium for electrically open case (78) and electrically short case (79) reduce to

$$|a_{ij}|_{11 \times 11} = 0, \quad \forall i, j = 1, 2, ..11 \qquad (80)$$

and

$$|b_{ij}|_{9 \times 9} = 0, \quad \forall i, j = 1, 2, ..9 \qquad (81)$$

where a_{ij} and b_{ij} are defined in Appendix D.

Case 2 When the suggested model is simplified to a structure consisting only of a magneto-electro-elastic semi-infinite medium (i.e., $C_{44}^{(2)}$, $e_{15}^{(2)}$, $\kappa_{11}^{(2)}$, $\mu_{11}^{(2)}$, $\rho_2 = 0$), the dispersion relations for electrically open condition (equation (78)) and for electrically short condition (equation (79)) reduced to

$$|c_{mn}|_{5 \times 5} = 0, \quad \forall m, n = 1, 2, ..11 \qquad (82)$$

and

$$|d_{mn}|_{3 \times 3} = 0, \quad \forall m, n = 1, 2, ..9 \qquad (83)$$

where c_{mn} and d_{mn} are defined in Appendix E. The dispersion relations (equations (82) and (83)) are in good agreement with the results obtained by Li et al. [11].

7. Numerical results and discussion

In this investigation, we consider two cases, i.e. electrically open case and electrically short case.

A function of wave number is used to describe the influence on the phase velocity of the initial stress. For this study, we utilize the piezoelectric material BaTiO₃, as referenced in the work of Cao et al. [25], and the magneto-electro-elastic material BaTiO₃-CoFe₂O₄, as studied by Li et al. [11]. The following Table 1 summarizes all of the material constants used in this article. $\kappa_0 = 8.85 \times 10^{-12}$ F/m and $\mu_0 = 4\pi \times 10^{-7}$ Ns^2C^{-2} are the dielectric constant and magnetic permittivity of vacuum, respectively.

The non-dimensional velocities of shear horizontal transverse waves in the functionally graded magneto-electro-elastic material layer and piezoelectric semi-infinite medium are represented as c_1 and c_2, respectively, and are expressed as follows:

$$c_1 = \sqrt{\frac{A_0}{\rho_{10}}} \text{ and } c_2 = \sqrt{\frac{B_0}{\rho_{20}}}$$

Graphical representations have been depicted to illustrate the influence of several key parameters, including the functional gradient parameters $\alpha_1 h$ and $\alpha_2 h$ associated with the layer and semi-infinite medium and the mechanical imperfection parameter $(\frac{K}{B^0})$, on the dimensionless phase velocity $(\frac{c}{c_1})$ of the propagating SH-wave relative to the dimensionless wave number (kh), for both electrically open and electrically short cases, as depicted in the corresponding figures.

7.1. Electrically open case

In this section, we visually represent the effects of the inhomogeneity parameters ($\alpha_1 h$, $\alpha_2 h$), depth (h), and mechanical interfacial imperfection bonding parameter $(\frac{K}{B^0})$ on phase velocity for the electrically open situation.
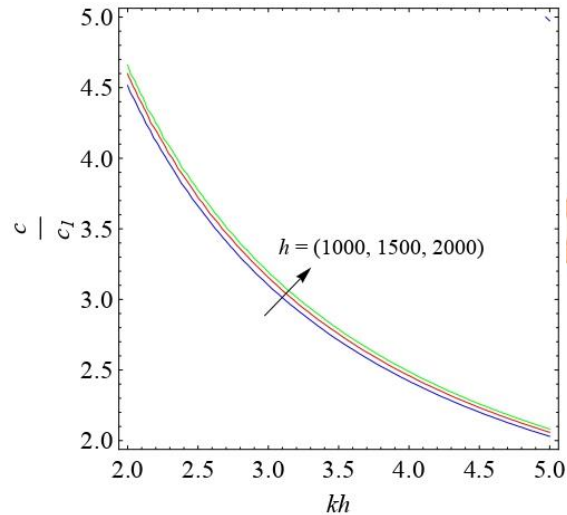

Figure 2: For varying values of h, the relationship between the non-dimensional phase velocity and the non-dimensional wave number for an electrically open case.
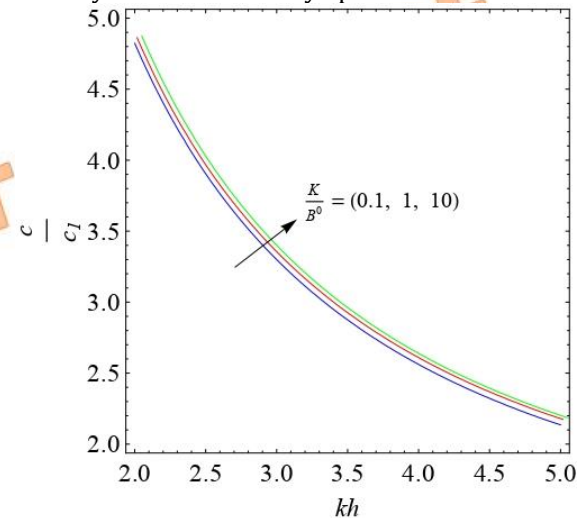

Figure 3: For varying values of K, the relationship between the non-dimensional phase velocity and the non-dimensional wave number for an electrically open case.

The electrically open case is pertinent only at the layer-vacuum interface. The electrically open situation refers to a specific boundary condition or scenario in which electromagnetic waves or electrical signals are not constrained or confined within a closed system or structure. In this case, there are no impedance mismatches or reflections of the waves at the boundaries, enabling the free transmission of electromagnetic energy. The variations in wave number and phase velocity are depicted in Figures 2 to 5. The material used in this study consists of a magneto-electro-elastic material BaTiO$_3$-CoFe$_2$O$_4$ and a piezoelectric material BaTiO$_3$. The wave number and phase velocity play significant roles in influencing the propagation of shear horizontal transverse waves in the considered structure. Figure 2 depicts the variation of phase velocity versus wave number for different depths, h (=1000, 1500, and 2000). It has been observed that, as the depth increases, the phase velocity increases.

Table 1: Material constants for BaTiO$_3$-CoFe$_2$O$_4$ [26] and BaTiO$_3$ [11]

Materials	Elastic constant $C_{44}(10^{10}\,\text{N/m}^2)$	Piezoelectric constant $e_{15}(\text{C/m}^2)$	Piezomagnetic constant h_{15} (N/Am)	Magnetic Constant $\mu_{11}(10^{-6}\,\text{Ns}^2\text{C}^{-2})$	Dielectric constant $\kappa_{11}(10^{-9}\,\text{C/Vm})$	Magnetoelectric constant $\beta_{11}(10^{-9}\,\text{Ns/VC})$	Mass density ρ (10^3 kg/m^3)
BaTiO$_3$-CoFe$_2$O$_4$	4.8	0.08	238	−258	0.19	0.005	7.50
BaTiO$_3$	4.4	11.4	–	5	9.86	–	5.7

This observed behavior carries significant physical implications, suggesting that an increase in the depth of the material or structure is associated with a higher speed of wave propagation.
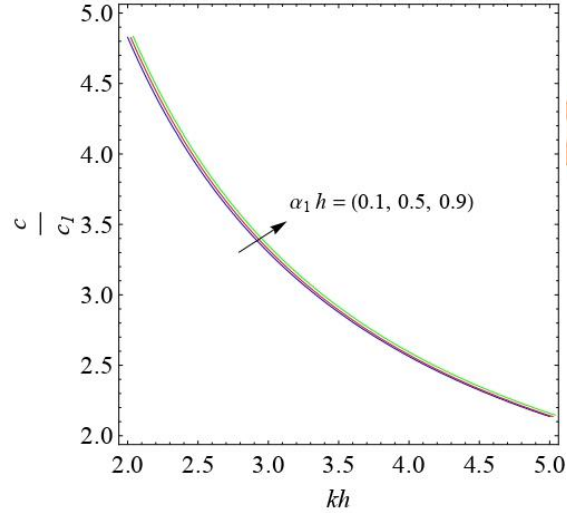
including wave amplitude, phase, and dispersion properties at the material or layer interface. The graph clearly demonstrates that the phase velocity increases proportionally with an increase in $\frac{K}{B^0}$.
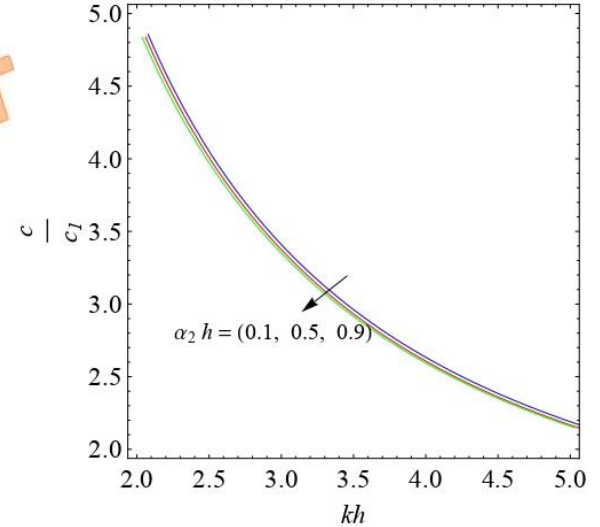

Figure 4: For varying values of α_1, the relationship between the non-dimensional phase velocity and the non-dimensional wave number for an electrically open case.

Figure 5: For varying values of α_2, the relationship between the non-dimensional phase velocity and the non-dimensional wave number for an electrically open case.

Such a phenomenon might be linked to changes in material properties, potentially indicating that thinner layers exhibit enhanced stiffness or density. Figure 3 depicts the impact of different interfacial imperfection bonding parameters $\frac{K}{B^0}$ (= 0.1, 1, 10) GPa on the relationship between phase velocity and wave number. The mechanically interfacial imperfection bonding parameter plays a crucial role in wave transmission, reflection, and scattering phenomena at the interface, influencing various propagation characteristics,

Figures 4 and 5 provide insights into the impact of the inhomogeneity parameters, represented by parameters $\alpha_1 h$ for layer and $\alpha_2 h$ for semi-infinite medium, on the relationship between phase velocity and wave number. The curves in Figure 4 show that raising the values of inhomogeneity parameter $\alpha_1 h$ increases the phase velocity of shear horizontal transverse type wave. In Figure 5, increasing the value of inhomogeneity parameter $\alpha_2 h$ decreases the phase velocity of a shear horizontal transverse type wave. By manipulating the inhomogeneity

parameter, researchers can analyze and model the impact of material variations on wave propagation, facilitating a more comprehensive understanding of wave behavior in inhomogeneous media.
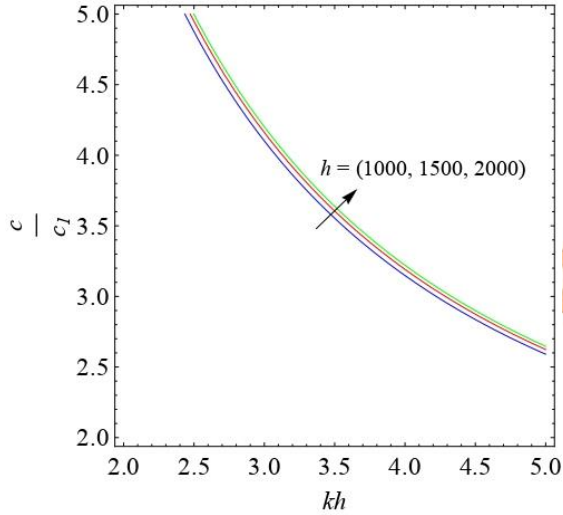

Figure 6: For varying values of h, the relationship between the non-dimensional phase velocity and the non-dimensional wave number for an electrically short case.

This knowledge is essential for customizing materials and comprehending how waves behave, especially in fields like materials engineering and structural design

7.2. Electrically short case

Similar to the electrically open case, this study also examined a configuration involving the magneto-electro-elastic material BaTiO$_3$-CoFe$_2$O$_4$ and the piezoelectric material BaTiO$_3$ for the electrically short case. This section investigates how the depth (h), mechanical interfacial imperfection bonding parameter ($\frac{K}{B^0}$), and inhomogeneity parameters ($\alpha_1 h$ and $\alpha_2 h$) impact the phase velocity in the electrically short scenario. In an electrically short case, the system or structure being studied is characterized by its small physical size compared to the wavelength

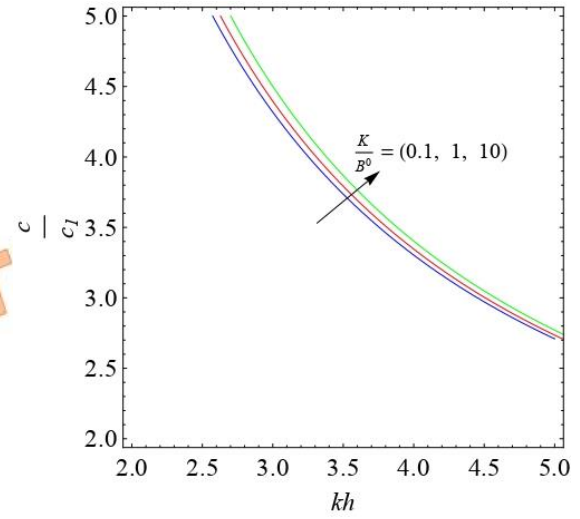of the electromagnetic waves or electrical signals with which it interacts.

Figure 7: For varying values of K, the relationship between the non-dimensional phase velocity and the non-dimensional wave number for an electrically short case.

This condition has implications for understanding the behavior of electrical signals and making appropriate considerations for impedance matching, signal transmission, and electromagnetic wave propagation. Figures 6 to 9 provide insights into how these parameters influence the characteristics of wave propagation. Figure 6 illustrates the observed variations for different values of h (= 1000, 1500, and 2000), portraying the relationship between phase velocity and wave number. The graph unambiguously illustrates that the phase velocity shows a proportional increase with an increment in-depth h. Subsequently, Figure 7 illustrates the influence of various values of $\frac{K}{B^0}$ on the relationship between phase velocity and wave number. The mechanical interfacial imperfection bonding parameter plays a critical role in wave transmission,

Table 2: Summary of the effect of parameters on phase velocity

Parameters	Effect on phase velocity for electrically open case	Effect on phase velocity for electrically short case
Depth (h)	Direct proportion	Direct proportion
Mechanically interfacial imperfect interface (K)	Direct proportion	Direct proportion
Material gradient parameter for layer (α_1)	Direct proportion	Direct proportion
Material gradient parameter for semi-infinite medium (α_2)	Inverse proportion	Inverse proportion

12

reflection, and scattering phenomena at the interface, impacting several propagation characteristics such as wave amplitude, phase, and dispersion properties at the material or layer interface. The graph demonstrates that the phase velocity increases with an increase in $\frac{K}{B^0}$. Figures 8 and 9 show the phase velocity versus wave number for various values of the material gradient parameters for layer $\alpha_1 h$ (= 0.1, 0.5, 0.9) and for semi-infinite medium $\alpha_2 h$ (= 0.1, 0.5, 0.9). As seen in the open case, the phase velocity increases as the value of the material gradient parameter $\alpha_1 h$ increases and the phase velocity decreases as the value of the inhomogeneity parameter $\alpha_2 h$ increases. Grasping this connection is vital for customizing materials with precise gradient profiles and enhancing their effectiveness in fields such as materials engineering and structural design. The effect of these parameters on phase velocity is summarised in Table 2.

8. Conclusions

This study has offered valuable insights into the propagation behavior of shear horizontal transverse waves in a functionally graded magneto-electro-elastic layer and a piezoelectric semi-infinite medium. By considering various parameters such as depth h, interfacial imperfection bonding parameter $\frac{K}{B^0}$, and inhomogeneity parameters $\alpha_1 h$ and $\alpha_2 h$, we have gained a comprehensive understanding of the factors influencing the phase velocity of shear horizontal waves in both electrically open and short scenarios.
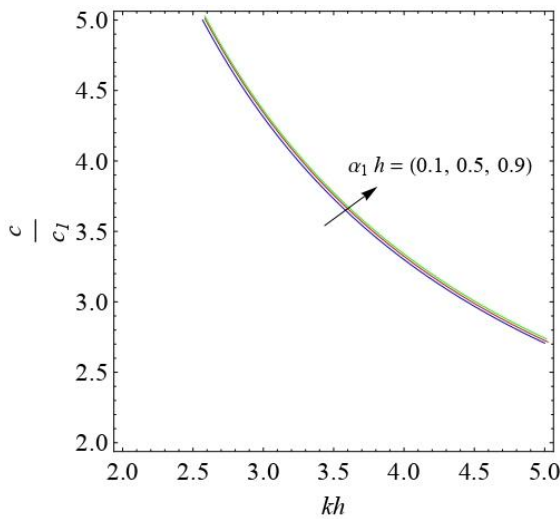
(1) Throughout the study, a significant observation can be made that the phase velocity of the shear horizontal transverse waves increases with the decreasing magnitude of the wave number, as is evident in all the figures.

(2) The depth h of the layer has emerged as an influential factor, affecting the phase velocity in both electrically open and short cases. As the depth increases, the phase velocity of shear horizontal transverse waves increases, indicating the importance of considering the layer's thickness in wave propagation analysis.

(3) The mechanically interfacial imperfection bonding parameter associated with the magneto-electro-elastic layer and piezoelectric semi-infinite medium affects the phase velocity of shear horizontal transverse waves directly. Specifically, an increase in the mechanical interfacial imperfection bonding parameter increases the phase velocity for both electrically open and electrically short cases, further emphasizing its influence on wave propagation characteristics.

(4) The phase velocity of the shear horizontal transverse wave is also influenced by the material gradient parameter of the upper boundary, and it increases with the rising value of the material gradient parameter of the upper boundary for both electrically short and electrically open cases.

(5) The phase velocity of a shear horizontal transverse wave is also influenced by the material gradient parameter of a functionally graded piezoelectric semi-infinite medium, and it decreases with the rising value of the inhomogeneity parameter of a functionally graded piezoelectric semi-infinite medium for both electrically short and electrically open cases.
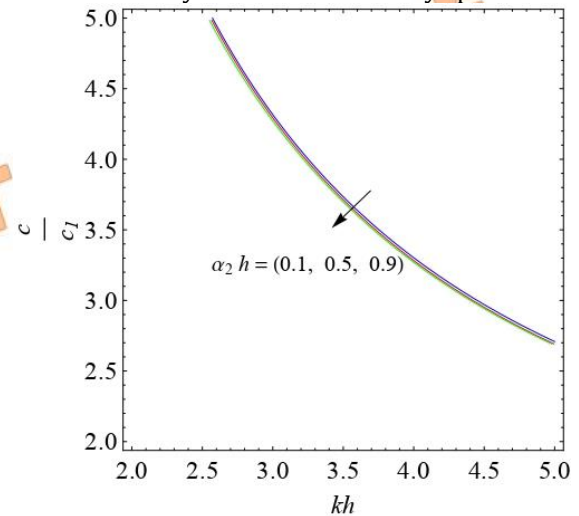

Figure 8: For varying values of α_1, the relationship between the non-dimensional phase velocity and the non-dimensional wave number for an electrically short case.

Figure 9: For varying values of α_2, the relationship between the non-dimensional phase velocity and the non-dimensional wave number for an electrically short case.

(6) The consequences of the study presented here find their application in the production and development of SAW devices. SAW devices that rely on the transduction of acoustic waves include filters, oscillators, and transformers. The transduction of electric energy into mechanical energy is accomplished by the use of piezoelectric materials. The SAW device is also used in radio and television, quantum acoustics, and geophysics.

(7) The findings of this research significantly contribute to engineering fields, especially in shear horizontal transverse wave propagation in layered structures. The proposed model of a functionally graded magneto-electro-elastic layer and piezoelectric semi-infinite medium provides versatile and adaptable sensing capabilities for diverse applications. In electric power equipment, the model's sensitivity to electromagnetic fields enables precise monitoring and anomaly detection.

Acknowledgments

Funding Statement

Conflicts of Interest

The author declares that there is no conflict of interest regarding the publication of this article.

Appendixes

Appendix A

$$d_1 = 1 + \alpha_1 h,$$

$$f_1 = k\sqrt{\frac{\rho_{10}c^2}{A^0} - 1} + \frac{\alpha_1^2}{8k}\sqrt{\frac{A^0}{\rho_{10}c^2 - A^0}},$$

$$f_2 = k - \frac{\alpha_1^2}{8k},$$

$$f_3 = k\sqrt{\frac{\rho_{10}c^2}{A^0} - 1} + \frac{\alpha_1^2}{8kd_1^2}\sqrt{\frac{A^0}{\rho_{10}c^2 - A^0}},$$

$$f_4 = k - \frac{\alpha_1^2}{8kd_1^2},$$

$$f_5 = k\sqrt{\frac{\rho_{20}c^2}{B^0} - 1} + \frac{\alpha_2^2}{8k}\sqrt{\frac{B^0}{\rho_{20}c^2 - B^0}},$$

$$f_6 = k - \frac{\alpha_2^2}{8k},$$

$$p_1 = -kh\sqrt{\frac{\rho_{10}c^2}{A^0} - 1} - \frac{\alpha_1}{8k}\sqrt{\frac{A^0}{\rho_{10}c^2 - A^0}},$$

$$p_2 = -kh + \frac{\alpha_1}{8k},$$

$$p_3 = -\frac{\alpha_1}{8k}\sqrt{\frac{A^0}{\rho_{10}c^2 - A^0}}, \quad p_4 = \frac{\alpha_1}{8k},$$

$$p_5 = -\frac{\alpha_2}{8k}\sqrt{\frac{B^0}{\rho_{20}c^2 - B^0}}, \quad p_6 = \frac{\alpha_2}{8k},$$

$$m^0 = e_{15}^{10} - \kappa_{11}^{10}a_2 - \beta_{11}^{10}a_3,$$

$$l^0 = h_{15}^{10} - \beta_{11}^{10}a_2 - \mu_{11}^{10}a_3.$$

Appendix B

$$r_{11} = A^0\left(\frac{-\alpha_1}{2} + if_1\right)e^{ip_1},$$

$$r_{12} = -A^0\left(\frac{\alpha_1}{2} + if_1\right)e^{-ip_1},$$

$$r_{13} = e_{15}^{10}\left(\frac{-\alpha_1}{2} + f_2\right)e^{p_2},$$

$$r_{14} = -e_{15}^{10}\left(\frac{\alpha_1}{2} + f_2\right)e^{-p_2},$$

$$r_{15} = h_{15}^{10}\left(\frac{-\alpha_1}{2} + f_2\right)e^{p_2},$$

$$r_{16} = -h_{15}^{10}\left(\frac{\alpha_1}{2} + f_2\right)e^{-p_2},$$

$$r_{17} = r_{18} = r_{19} = r_{110} = r_{111} = 0.$$

$$r_{21} = a_2 e^{ip_1}, \quad r_{22} = a_2 e^{-ip_1}, \quad r_{23} = e^{p_2},$$

$$r_{24} = e^{-p_2}, \quad r_{25} = r_{26} = r_{27} = r_{28} = r_{29} = 0,$$

$$r_{210} = -e^{-kh}, \quad r_{211} = 0.$$

$$r_{31} = m^0\left(\frac{-\alpha_1}{2} + if_1\right)e^{ip_1},$$

$$r_{32} = -m^0\left(\frac{\alpha_1}{2} + if_1\right)e^{-ip_1},$$

$$r_{33} = -\kappa_{11}^{10}\left(\frac{-\alpha_1}{2} + f_2\right)e^{p_2},$$

$$r_{34} = \kappa_{11}^{10}\left(\frac{\alpha_1}{2} + f_2\right)e^{-p_2},$$

$$r_{35} = -\beta_{11}^{10}\left(\frac{-\alpha_1}{2} + f_2\right)e^{p_2},$$

$$r_{36} = \beta_{11}^{10}\left(\frac{\alpha_1}{2} + f_2\right)e^{-p_2},$$

$$r_{37} = r_{38} = r_{39} = 0, \quad r_{310} = \kappa_0 k e^{-kh}, \quad r_{311} = 0.$$

$$r_{41} = a_3 e^{ip_1}, \quad r_{42} = a_3 e^{-ip_1}, \quad r_{43} = r_{44} = 0,$$

$$r_{45} = e^{p_2}, \quad r_{46} = e^{-p_2}, \quad r_{47} = r_{48} = r_{49} = r_{410} = 0, \quad r_{411} = -e^{-kh}.$$

$r_{51} = l^0(\frac{-\alpha_1}{2} + if_1)e^{ip_1},$

$r_{52} = -l^0(\frac{\alpha_1}{2} + if_1)e^{-ip_1},$

$r_{53} = \beta_{11}^{10}(\frac{-\alpha_1}{2} + f_2)e^{p_2},$

$r_{54} = -\beta_{11}^{10}(\frac{\alpha_1}{2} + f_2)e^{-p_2},$

$r_{55} = \mu_{11}^{10}(\frac{-\alpha_1}{2} + f_2)e^{p_2},$

$r_{56} = -\mu_{11}^{10}(\frac{\alpha_1}{2} + f_2)e^{-p_2},$

$r_{57} = r_{58} = r_{59} = r_{510} = 0, r_{511} = \mu_0 k e^{-kh}.$

$r_{61} = A^0 d_1(\frac{-\alpha_1}{2d_1} + i\sqrt{d_1}f_3)e^{ip_3},$

$r_{62} = -A^0 d_1(\frac{\alpha_1}{2d_1} + i\sqrt{d_1}f_3)e^{-ip_3},$

$r_{63} = e_{15}^{10} d_1(\frac{-\alpha_1}{2d_1} + \sqrt{d_1}f_4)e^{p_4},$

$r_{64} = -e_{15}^{10} d_1(\frac{\alpha_1}{2d_1} + \sqrt{d_1}f_4)e^{-p_4},$

$r_{65} = h_{15}^{10} d_1(\frac{-\alpha_1}{2d_1} + \sqrt{d_1}f_4)e^{p_4},$

$r_{66} = -h_{15}^{10} d_1(\frac{\alpha_1}{2d_1} + \sqrt{d_1}f_4)e^{-p_4},$

$r_{67} = B^0(\frac{\alpha_2}{2} + if_5)e^{-ip_5}, r_{68} = e_{15}^1(\frac{\alpha_2}{2} + f_6)e^{-p_6},$
$\quad r_{69} = r_{610} = r_{611} = 0.$

$r_{71} = \frac{-K}{\sqrt{d_1}}e^{ip_3}, r_{72} = -\frac{K}{\sqrt{d_1}}e^{-ip_3},$

$r_{73} = r_{74} = r_{75} = r_{76} = 0,$

$r_{77} = (-B^0(\frac{\alpha_2}{2} + if_5) + K)e^{-ip_5},$

$r_{78} = -e_{15}^{20}(\frac{\alpha_2}{2} + f_6)e^{-p_6}, r_{79} = r_{710} = r_{711} = 0.$

$r_{81} = \frac{a_2}{\sqrt{d_1}}e^{ip_3}, r_{82} = \frac{a_2}{\sqrt{d_1}}e^{-ip_3}, r_{83} = \frac{1}{\sqrt{d_1}}e^{p_4},$

$r_{84} = \frac{1}{\sqrt{d_1}}e^{-p_4}, r_{85} = r_{86} = 0, r_{87} = -\frac{e_{15}^1}{\kappa_{11}^1}e^{-ip_5},$

$r_{88} = -e^{-p_6}, r_{89} = r_{810} = r_{811} = 0.$

$r_{91} = \frac{a_3}{\sqrt{d_1}}e^{ip_3}, r_{92} = \frac{a_3}{\sqrt{d_1}}e^{-ip_3}, r_{93} = r_{94} = 0,$

$r_{95} = \frac{1}{\sqrt{d_1}}e^{p_4}, r_{96} = \frac{1}{\sqrt{d_1}}e^{-p_4}, r_{97} = r_{98} = 0,$

$r_{99} = -e^{-p_6}, r_{910} = r_{911} = 0.$

$r_{1001} = m^0 d_1(\frac{-\alpha_1}{2d_1} + i\sqrt{d_1}f_3)e^{ip_3},$

$r_{1002} = -m^0 d_1(\frac{\alpha_1}{2d_1} + i\sqrt{d_1}f_3)e^{-ip_3},$

$r_{1003} = -\kappa_{11}^0 d_1\left(\frac{-\alpha_1}{2d_1} + \sqrt{d_1}f_4\right)e^{p_4}, r_{1004} =$
$\kappa_{11}^{10} d_1(\frac{\alpha_1}{2d_1} + \sqrt{d_1}f_4)e^{-p_4},$

$r_{1005} = r_{1006} = r_{1007} = 0,$

$r_{1008} = \kappa_{11}^1(\frac{\alpha_2}{2} + f_6)e^{-p_6},$

$r_{1009} = r_{1010} = r_{1011} = 0.$

$r_{1101} = l^0 d_1(\frac{-\alpha_1}{2d_1} + i\sqrt{d_1}f_3)e^{ip_3},$

$r_{1102} = -l^0 d_1(\frac{\alpha_1}{2d_1} + i\sqrt{d_1}f_3)e^{-ip_3},$

$r_{1103} = \beta_{11}^0 d_1(\frac{-\alpha_1}{2d_1} + \sqrt{d_1}f_4)e^{p_4},$

$r_{1104} = -\beta_{11}^0 d_1(\frac{\alpha_1}{2d_1} + \sqrt{d_1}f_4)e^{-p_4},$

$r_{1105} = -\mu_{11}^0 d_1(\frac{-\alpha_1}{2d_1} + \sqrt{d_1}f_4)e^{p_4},$

$r_{1106} = \mu_{11}^0 d_1(\frac{\alpha_1}{2d_1} + \sqrt{d_1}f_4)e^{-p_4},$

$r_{1107} = r_{1108} = 0,$

$r_{1109} = -\mu_{11}^1(\frac{\alpha_2}{2} + f_6)e^{-p_6}, r_{1110} = r_{1111} = 0.$

Appendix C

$\boldsymbol{r_{ij} = t_{mn}}$

$\forall i = 1,6,7,8,9,10,11; j = 1,2,..,9;$

$m = 1,4,5,6,7,8,9; n = 1,2,..,9.$

$t_{21} = a_2 e^{ip_1}, t_{22} = a_2 e^{-ip_1}, t_{23} = e^{p_2},$

$t_{24} = e^{-p_2}, t_{25} = t_{26} = t_{27} = t_{28} = t_{29} = 0.$

$t_{31} = a_3 e^{ip_1}, t_{32} = a_3 e^{-ip_1}, t_{33} = t_{34} = 0,$

$t_{35} = e^{p_2}, t_{36} = e^{-p_2}, t_{37} = t_{38} = t_{39} = 0.$

Appendix D

$\boldsymbol{r_{ij} = a_{ij},}$

$\boldsymbol{\forall i = 1, ..., 6,, 8, ..., 11; j = 1, 2, .., 9,}$

$a_{71} = \frac{-1}{\sqrt{d_1}}e^{ip_3}, a_{72} = \frac{-1}{\sqrt{d_1}}e^{-ip_3},$

$a_{73} = a_{74} = a_{75} = a_{76} = 0,$

$a_{77} = e^{-ip_5}, a_{78} = a_{79} = a_{710} = a_{711} = 0.$

$t_{ij} = b_{ij}$

$\forall i = 1, ..., 6,, 8, .., 11; j = 1,2,..,9;$

$a_{ij} = b_{ij} \quad \forall i = 7; j = 1,2,..,9.$

Appendix E

$\boldsymbol{r_{ij} = c_{mn}, \forall i = 1, 2, 3, 4, 5; j = 1, 2, 3, 10, 11;}$

$$m = 1,2,3,4,5; n = 1,2,3,4,5.$$

$$t_{ij} = d_{mn} \quad \forall i = 1,6,7; \; j = 1,2,3;$$

$$m = 1,2,3; n = 1,2,3.$$

References

1] Liu, B., Chen, X., Cai, H., Ali, M.M., Tian, X., Tao, L., Yang, Y. and Ren, T., 2016. Surface acoustic wave devices for sensor applications. *Journal of semiconductors*, *37*(2), p.021001.

[2] Wells, P.N., 2006. Ultrasound imaging. *Physics in medicine & biology*, *51*(13), p.R83.

[3] Golchin Khazari, S., Mohammadi, Y. and Kheirikhah, M.M., 2023. Investigation of Properties and Application of Magneto Electro Elastic Materials and Analysis of Piezoelectric Smart Shells. *Transactions of the Indian Institute of Metals*, *76*(11), pp.2915-2929.

[4] Li, L. and Wei, P.J., 2014. The piezoelectric and piezomagnetic effect on the surface wave velocity of magneto-electro-elastic solids. *Journal of Sound and Vibration*, *333*(8), pp.2312-2326.

[5] Chen, J., Pan, E. and Chen, H., 2007. Wave propagation in magneto-electro-elastic multilayered plates. *International Journal of Solids and Structures*, *44*(3-4), pp.1073-1085.

[6] Chen, J., Guo, J. and Pan, E., 2017. Wave propagation in magneto-electro-elastic multilayered plates with nonlocal effect. *Journal of Sound and Vibration*, *400*, pp.550-563.

[7] Akshaya, A., Kumar, S. and Hemalatha, K., 2024. Transference of SH-Waves in Two Different Functionally Graded Half-Spaces. *Mechanics of Solids*, pp.1-22.

[8] Liu, J.X., Fang, D.N., Wei, W.Y. and Zhao, X.F., 2008. Love waves in layered piezoelectric/piezomagnetic structures. *Journal of Sound and Vibration*, *315*(1-2), pp.146-156.

[9] Akshaya, A., Kumar, S. and Hemalatha, K., 2024. Behavior of Transverse Wave at an Imperfectly Corrugated Interface of a Functionally Graded Structure. *Physics of Wave Phenomena*, *32*(2), pp.117-134.

[10] Yang, J., 2008. X. Li. SH Wave Scattering on Cracks in Functionally Graded Piezoelectric/Piezomagnetic Materials. *Chinese Journal of Applied Mechanics*, *25*, pp.279-284.

[11] Li, L. and Wei, P.J., 2014. Surface wave speed of functionally graded magneto-electro-elastic materials with initial stresses. *Journal of Theoretical and Applied Mechanics*, *44*(3), pp.49-64.

[12] Hemalatha, K., Kumar, S. and Kim, I., 2023. Study of SH-wave in a pre-stressed anisotropic magnetoelastic layer sandwich by heterogeneous semi-infinite media. *Mathematics and Computers in Simulation*.

[13] Cao, X., Jin, F., Jeon, I. and Lu, T.J., 2009. Propagation of Love waves in a functionally graded piezoelectric material (FGPM) layered composite system. *International Journal of Solids and Structures*, *46*(22-23), pp.4123-4132.

[14] Du, J., Jin, X., Wang, J. and Xian, K., 2007. Love wave propagation in functionally graded piezoelectric material layer. *Ultrasonics*, *46*(1), pp.13-22.

[15] Hua, L.I.U., YANG, J.L. and LIU, K.X., 2007. Love waves in layered graded composite structures with imperfectly bonded interface. *Chinese Journal of Aeronautics*, *20*(3), pp.210-214.

[16] Li, X.Y., Wang, Z.K. and Huang, S.H., 2004. Love waves in functionally graded piezoelectric materials. *International Journal of Solids and Structures*, *41*(26), pp.7309-7328.

[17] Eskandari, M. and Shodja, H.M., 2008. Love waves propagation in functionally graded piezoelectric materials with quadratic variation. *Journal of Sound and Vibration*, *313*(1-2), pp.195-204.

[18] Akshaya, A., Kumar, S., Prasad, K. and Majhi, D., 2024. Transference of shear horizontal waves in a functionally graded piezoelectric structure. *Partial Differential Equations in Applied Mathematics*, p.100725.

[19] Saroj, P.K., Sahu, S.A., Chaudhary, S. and Chattopadhyay, A., 2015. Love-type waves in functionally graded piezoelectric material (FGPM) sandwiched between initially stressed layer and elastic substrate. *Waves in Random and Complex Media*, *25*(4), pp.608-627.

[20] Singh, A.K., Parween, Z. and Kumar, S., 2016. Love-type wave propagation in a corrugated piezoelectric structure. *Journal of Intelligent Material Systems and Structures*, *27*(19), pp.2616-2632.

[21] Majhi, S., Pal, P.C. and Kumar, S., 2016. Love waves in a layered functionally graded piezoelectric structure under initial stress. *Waves in Random and Complex Media*, *26*(4), pp.535-552.

[22] Sahu, S.A., Mondal, S. and Dewangan, N., 2019. Polarized shear waves in functionally graded piezoelectric material layer sandwiched between corrugated piezomagnetic layer and elastic substrate. *Journal of Sandwich Structures & Materials*, *21*(8), pp.2921-2948.

[23] Liu, G.R., Han, X. and Lam, K.Y., 1999. Stress waves in functionally gradient materials and its use for material characterization. *Composites Part B: Engineering*, *30*(4), pp.383-394.

[24] Liu, Y., Lin, S., Li, Y., Li, C. and Liang, Y., 2019. Numerical investigation of Rayleigh waves in layered composite piezoelectric structures using the SIGA-PML approach. *Composites Part B: Engineering*, *158*, pp.230-238.

[25] Cao, X., Shi, J. and Jin, F., 2012. Lamb wave propagation in the functionally graded piezoelectric–piezomagnetic material plate. *Acta Mechanica*, *223*(5), pp.1081-1091.

[26] Hemalatha, K., Kumar, S. and Prakash, D., 2023. Dispersion of Rayleigh wave in a functionally graded piezoelectric layer over elastic substrate. *Forces in Mechanics*, *10*, p.100171.

[27] Sadab, M. and Kundu, S., 2023. SH-wave propagation in a piezoelectric layer over a heterogeneous dry sandy half-space. *Acta Mechanica*, *234*(11), pp.5841-5854.

[28] Hemalatha, K., Kumar, S. and Akshaya, A., 2023. Rayleigh wave at imperfectly corrugated interface in FGPM structure. *Coupled Systems Mechanics*, *12*(4), p.337.

[29] Singh, S.S., 2011. Love wave at a layer medium bounded by irregular boundary surfaces. *Journal of Vibration and Control*, *17*(5), pp.789-795.

[30] Singh, S.S., 2011. Response of shear wave from a corrugated interface between elastic solid/viscoelastic half-spaces. *International Journal for Numerical and Analytical Methods in Geomechanics*, *35*(5), pp.529-543.

[31] Singh, A.K., Mistri, K.C., Kaur, T. and Sharma, S., 2017, January. Propagation of shear wave at a loosely bonded corrugated interface between a fibre-reinforced layer and an isotropic half-space. In *AIP Conference Proceedings* (Vol. 1802, No. 1). AIP Publishing.

[32] Lavrentyev, A.I. and Rokhlin, S.I., 1998. Ultrasonic spectroscopy of imperfect contact interfaces between a layer and two solids. *The Journal of the Acoustical Society of America*, *103*(2), pp.657-664.

[33] Karmakar, S., Sahu, S.A. and Goyal, S., 2022. Analyzis of wave scattering at the loosely bonded common interface of piezothermoelastic and isotropic elastic media under LS (Lord-Shulman) and GL (Green-Lindsay) theory of thermoelasticity. *Journal of Thermal Stresses*, *45*(2), pp.117-138.

[34] Wang, X., Pan, E. and Roy, A.K., 2007. Scattering of antiplane shear wave by a piezoelectric circular cylinder with an imperfect interface. *Acta mechanica*, *193*(3-4), pp.177-195.

[35] Singh, A.K., Lakshman, A., Mistri, K.C. and Pal, M.K., 2018. Torsional surface wave propagation in an imperfectly bonded corrugated initially-stressed poroelastic sandwiched layer. *Journal of Porous Media*, *21*(6).

[36] Fröman, N. and Fröman, P.O., 2002. *Physical problems solved by the phase-integral method*. Cambridge University Press.

[37] Liu, J. and Wang, Z.K., 2004. The propagation behavior of Love waves in a functionally graded layered piezoelectric structure. *Smart Materials and Structures*, *14*(1), p.137.

[38] Jones, W., 1992. The application of the WKB approximation to the calculation of the scattering of radio waves from overdense meteor trains. *Planetary and space science*, *40*(11), pp.1487-1497.

[39] Cerveny, V. and Ravindra, R., 1973. Theory of seismic head waves. *American Journal of Physics*, *41*(5), pp.755-757.

[40] Qian, Z.H., Jin, F., Kishimoto, K. and Lu, T., 2009. Propagation behavior of Love waves in a functionally graded half-space with initial stress. *International Journal of Solids and Structures*, *46*(6), pp.1354-1361.

[41] Kumar, P., Mahanty, M., Chattopadhyay, A. and Singh, A.K., 2019. Effect of interfacial imperfection on shear wave propagation in a piezoelectric composite structure: Wentzel–Kramers–Brillouin asymptotic approach. *Journal of Intelligent Material Systems and Structures*, *30*(18-19), pp.2789-2807.

[42] Singhal, A., Sahu, S.A. and Chaudhary, S., 2018. Approximation of surface wave frequency in piezo-composite structure. *Composites Part B: Engineering*, *144*, pp.19-28.